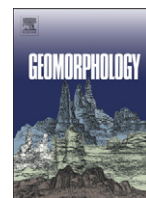




Contents lists available at ScienceDirect

Geomorphology

journal homepage: www.elsevier.com/locate/geomorph

Discrimination of fluvial, eolian and neotectonic features in a low hilly landscape: A DEM-based morphotectonic analysis in the Central Pannonian Basin, Hungary

Zsófia Ruzsiczay-Rüdiger^{a,*}, László Fodor^b, Erzsébet Horváth^{a,1}, Tamás Telbisz^{a,1}

^a Eötvös University, Institute of Geography and Earth Sciences, Department of Physical Geography, 1117 Budapest, Pázmány P. sétány 1/c, Hungary

^b Geological Institute of Hungary, 1143 Budapest Stefánia út 14, Hungary

ARTICLE INFO

Article history:

Received 19 September 2006

Received in revised form 7 August 2008

Accepted 28 August 2008

Available online xxxxx

Keywords:

Morphometry

Neotectonics

Drainage pattern analysis

Deflation

Pannonian Basin

Quaternary

ABSTRACT

The Gödöllő Hills, a low-relief terrain within the Central Pannonian Basin in Hungary, is characterised by moderate tectonic deformation rates. Although typical tectonic landforms are not clearly recognisable in the study area, this paper succeeded in discriminating between tectonically controlled landforms and features shaped by fluvial erosion or deflation with no tectonic control.

DEM-based morphometric parameters including elevation, slope and surface roughness, enabled the delineation of two NW–SE trending spearhead-shaped ridges separated by a wide rectilinear valley of the same strike. Although directional statistics suggested possible tectonic control of NW–SE striking landforms, precise morphometry completed with an analysis of subsurface structures rejected their tectonic preformation. Deflation plays a significant role in shaping the area, and the presence of two large-scale yardangs separated by a wind channel is proposed. In temperate-continental areas of Europe, no deflationary landforms of such scale have been described so far, suggesting that Pleistocene wind power in periglacial areas was more significant than it was previously thought.

Characteristic drainage patterns and longitudinal valley profiles enabled the recognition of areas probably affected by neotectonic deformation. A good agreement was observed between locations of Quaternary warping predicted by the morphometric study and subsurface structures revealed by the tectonic analysis. Zones of surface uplift and subsidence corresponded to anticlinal and synclinal hinges of fault-related folds. In low-relief and slowly-deforming areas, where exogenous forces may override tectonic deformation, only the integrated application of morphometric and subsurface-structural indications could assure correct interpretation of the origin of various landforms, while a morphometric study alone could have led to misinterpretation of some morphometric indices apparently suggesting tectonic preformation. On the other hand, the described morphological expression of subsurface structures could verify Quaternary age of the deformation.

© 2008 Elsevier B.V. All rights reserved.

1. Introduction

In low-relief regions distinction between landforms of different origin and recognition of features of neotectonic (Pliocene–Quaternary) deformation requires a complex array of methods. Morphotectonics is a relatively new direction in recognition of tectonic forces in landscape evolution (e.g. Burbank and Anderson, 2001; Keller and Pinter, 2002). The application of digital database, particularly the digital elevation models (DEM) permitted the quantitative characterisation of landforms (e.g. Burrough and McDonnell, 1998; Wilson and Gallant, 2000). Digitally assisted morphotectonics was successfully applied in tectonically active areas, like Taiwan, the western US, southern Italy or central Greece (Delcaillau, 2001; Scott and Pinter, 2003; Molin et al., 2004; Ganas et al., 2005). Here the relatively fast

deformation rate assures trustworthy connection of geomorphic indices and deformation features.

Low-relief landscapes may promote the recognition of tectonically controlled landforms, if the deformation rate is important. Holbrook and Schumm (1999) and Schumm et al. (2002) reported tectonically diverted drainage patterns on alluvial plains. However, conclusions on tectonic control of landforms drawn from morphotectonics are more problematic if the deformation rate is slow and/or the tectonic elements are not active during the last ca. 100 ky or the recurrence interval of phases of enhanced tectonic activity, like earthquakes is large (> 10 ky) with respect to the rate of exogenous processes. Low deformation rate, high accumulation rate by fluvial and/or eolian processes, high regional denudation rate, poor outcrop conditions are all factors that may decrease the power of morphotectonic analysis or prevent unambiguous conclusions. In such cases, a complex methodology – including “classical” geomorphic and geologic methods and novel digital techniques – is necessary, with the aim of understanding all aspects of the landscape evolution.

* Corresponding author. Tel.: +36 1 209 0555/1804; fax: +36 1 381 2112.

E-mail address: rzsofi@ludens.elte.hu (Z. Ruzsiczay-Rüdiger).

¹ fax: +36 1 381 2112.

The Pannonian Basin in Central Europe is characterised by low-relief, a considerable rate of active deformation confined to its western part ($<1.3 \text{ mm y}^{-1}$ shortening; [Greenrczy and Kenyeres, 2005](#)) coupled with an extensive late Pleistocene eolian sediment cover, which are hindering neotectonic and morphotectonic research. On the other hand, detailed geological mapping, broad history of “classical” geomorphological studies, long historical earthquake record ([Zsíros, 2000](#)) and good coverage of subsurface data partly counterbalance the disadvantages mentioned above. Particularly, a dense network of seismic reflection profiles permitted us to image the subsurface-structural pattern ([Fodor et al., 2005a](#), [Ruzsiczay-Rüdiger et al., 2007](#)) and discriminate between pre-neotectonic (pre-mid-Pliocene) and neotectonic structures. In this way, the conclusions based on geomorphic indices derived from the DEM analysis can be directly compared to a realistic tectonic pattern, in order to recognise potential tectonic control on landforms. This unique possibility to compare suspected structures with seismically imaged ones bears relevance for the applicability of morphotectonics in terrains similar to the Pannonian Basin. Additionally, the detailed geomorphological analysis can offer further discrimination on the origin of landforms, which do not seem to have deep-seated tectonic control but were formed by fluvial or eolian processes.

This paper is a tectonic–geomorphologic study of a hilly region of quasi-homogeneous lithology located in mid-latitude temperate climatic conditions. A novel combination of digital elevation data with subsurface structures provides a model for discriminating tectonic and non-tectonic landforms in a region of moderate deformation and significant fluvial and eolian activity during Quaternary times.

2. Geological and geomorphological setting

The Pannonian Basin is a low-altitude area surrounded by the Alps, Dinarides and Carpathians ([Fig. 1](#)). In the basin interior, uplifting basement of the mid-altitude Transdanubian Range (TR) separates two extended lowlands, the Danube Basin (DB) and the Great Hungarian Plain (GHP), characterised by ongoing subsidence. Simultaneous uplift and subsidence in the basin interior is typical of the neotectonic phase of the Pannonian Basin (late Pliocene–Quaternary) and is a consequence of compression induced by the continuous push of the Adriatic microplate after the closure of the Carpathian collision front ([Horváth and Cloetingh, 1996](#); [Bada et al., 1999, 2005](#)).

Our study area, the Gödöllő Hills, is located in the central part of the Pannonian Basin and is representative of the transitional zone between the uplifting TR and the subsiding GHP ([Fig. 1](#)). Pre-Tertiary basement is covered by Paleogene to middle Miocene sediments of variable thickness, which are exposed only in the northwest part of the Gödöllő Hills ([Rozlozsnik, 1936](#)). In its central and southeast parts, late Miocene (or Pannonian) to early Pliocene lacustrine and deltaic to fluvial sediments ([Uhrin and Sztanó, 2007](#)) reach 1000–1500 m in thickness ([Szentes, 1943](#); [Rónai, 1985](#)). The cross-bedded early Pliocene sandstone occurs typically on the N- and NW-facing, steep valley sides in the northern and central parts of the Gödöllő Hills ([Fig. 2](#)). These are covered unconformably with Quaternary sediments. The lack of major lithological differences indicates that local slope has been the most important control on development of the drainage network, which makes the area a promising target of a morphotectonic study.

The surface of the Gödöllő Hills is composed of two NW–SE trending, spearhead-shaped ridges (the Valkó and Úri Ridges), and a wide rectilinear valley, the Isaszeg Channel between them ([Fig. 2](#)). On the fluvially dissected surface of the ridges a loess–paleosol sequence of up to 40 m thickness has developed during the Quaternary. In the northern, most elevated part of the study area to the N of the town of Gödöllő on the Valkó Ridge and around Isaszeg in the Isaszeg Channel, eolian sand is characteristic ([Rozlozsnik, 1936](#); [Pávai Vajna, 1941](#); [Balla, 1959](#)) suggesting a significant role of deflation in the landscape evolution of the Gödöllő Hills. Some authors ([Szentes, 1943](#); [Balla, 1959](#)) connected specific landforms, (like linear valleys or sudden changes in flow direction) and the variable dip angles of outcropping upper Miocene–Pliocene layers to tectonic deformation. However, style and relative role of neotectonics and its complex interplay with fluvial and wind erosion have been poorly understood so far.

3. Methodology

Digital morphometry allows the quantification of topographic features, thus enables the objective comparison of different segments of the Earth's surface (e.g. [Pike, 1995](#)). DEMs are widely applied for the recognition and genetic classification of landforms ([Székely, 2001](#); [Scott and Pinter, 2003](#)), surface process modelling and tectonic geomorphology (e.g. [Zuchiewicz, 1991, 1998](#); [Demoulin, 1998](#); [Jordán, 2004](#); [Molin et al., 2004](#); [Jordán et al., 2005](#); [Ganas et al., 2005](#)). In this study, conventional methods of drainage pattern analysis (e.g. [Horton, 1945](#);

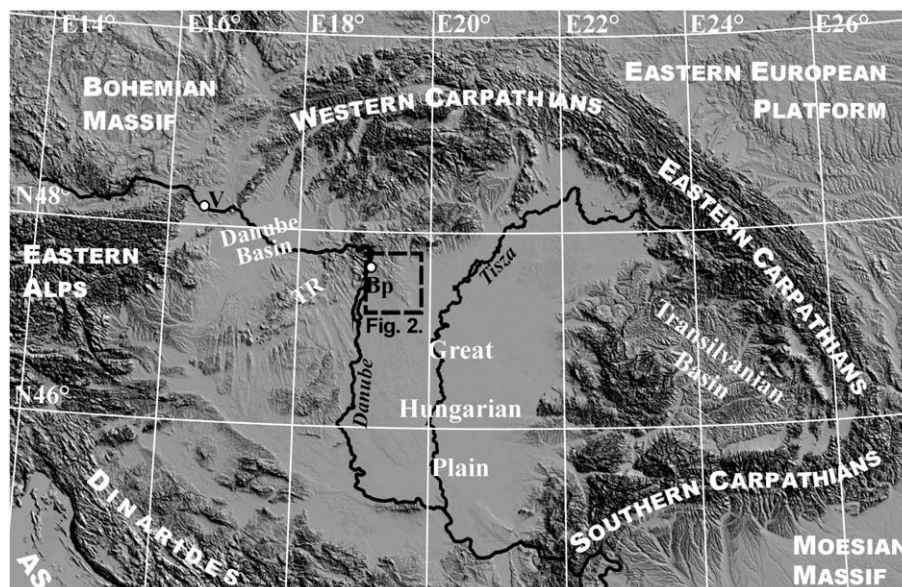


Fig. 1. Shaded relief map of the Pannonian Basin. AS: Adriatic Sea, Bp: Budapest, TR: Transdanubian Range, V: Vienna.

Strahler, 1952, 1957) and novel DEM techniques were employed jointly for the quantitative characterisation of surface morphology.

For the morphometric analysis the DEM called DDM-10 was employed, which is distributed by the Cartographic Institute of the Hungarian Ministry of Defence. DDM-10 is in EOVS projection system (Uniform National Projection System of Hungary); it has a horizontal cell size of 10 m and a vertical accuracy of 2.5 m. The DEM was processed and analysed using the ESRI ArcView 3.2 software. The rose diagrams were plotted by means of the GEOrient software.

DEM analysis was completed by a geologic and geomorphologic field study, which was essential for the correct interpretation of the DEM-derived data. Nevertheless, discussion of this is out of the scope of this study (see details in Ruszkiczay-Rüdiger, 2007). Investigation of tectonic structure was carried out using a net of industrial seismic reflection profiles. This morphotectonic study focuses on the possible surface expressions of neotectonic deformation, therefore applies the results of a detailed neotectonic study published by Ruszkiczay-Rüdiger et al. (2007) to confirm or reject tectonic control on certain landforms.

3.1. Morphometric parameters

Morphometry is defined as the quantitative measurement of landscape shape (Keller and Pinter, 2002), which allows the objective comparison of landforms. The formation of areas characterised by numerically different topography may be the consequence of geological, tectonic and/or climatic reasons (Székely, 2001). First step of the morphometric analysis of the Gödöllő Hills was the segmentation of the

study area. The quasi-homogeneous sub-areas were delineated by means of a quantitative analysis of the surface roughness, which characterises the spatial variability of elevation and slope parameters.

3.1.1. Elevation and slope

The DEM contains the coordinates and elevation above sea level of each cell of the study area (e.g. Carter, 1988). As a basic topographic parameter, which defines the runoff and local climate, the elevation is the starting point of all DEM-based morphometric analysis. The relief is the difference of elevation within a certain area ($h_{\max} - h_{\min}$). The relief in the Gödöllő Hills was analysed with neighbourhood statistics within a circular sampling window with a radius of 300 m.

The slope angle is the first derivative of the elevation data; it is the gradient (change of elevation at right angles to the contour-lines) across the study area independently from the elevation above sea level (e.g. Adediran et al., 2004). The “slope variability” refers to the difference between the minimum and maximum slope angle within a certain area ($\text{slope}_{\max} - \text{slope}_{\min}$). Similarly to the relief map, slope variability of the study area was also computed using neighbourhood statistics for a circular window of 300 m radius.

3.1.2. Delineation of drainage basins

The drainage divides were derived from the DEM using the *Basin extension* of the ArcView software. The *Basin Delineate* tool delineates a catchment from a point defined on a stream by the user. In the study area this point was the outlet of each stream, the place where it leaves its incised valley at the margin of the Gödöllő Hills.

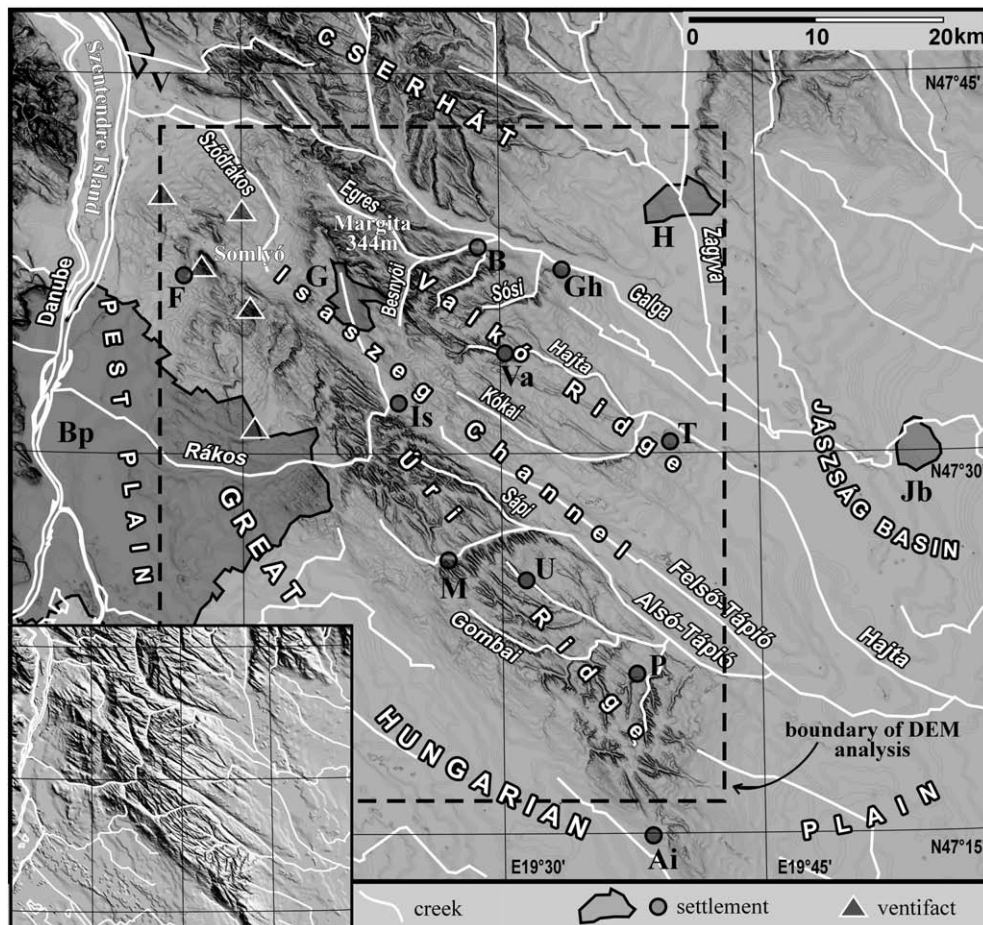


Fig. 2. Slope map of the Gödöllő Hills with major settlements, important geographic names and ventifact occurrences (after Jámber, 2002). On the base-map darker colours indicate steeper slopes (max. slope angle 25–30°). Small inset is the shaded relief map of the area. Note the gradual smoothing into the lowlands towards the E and the sharp, rectilinear edge in the SW. Ai: Albertirsa, B: Bag, Bp: Budapest, F: Fót, G: Gödöllő, Gh: Galgahévíz, H: Hatvan, Is: Isaszeg, Jb: Jászberény, M: Mende, P: Pánd, T: Tóalmás, U: Uri, Va: Valkó.

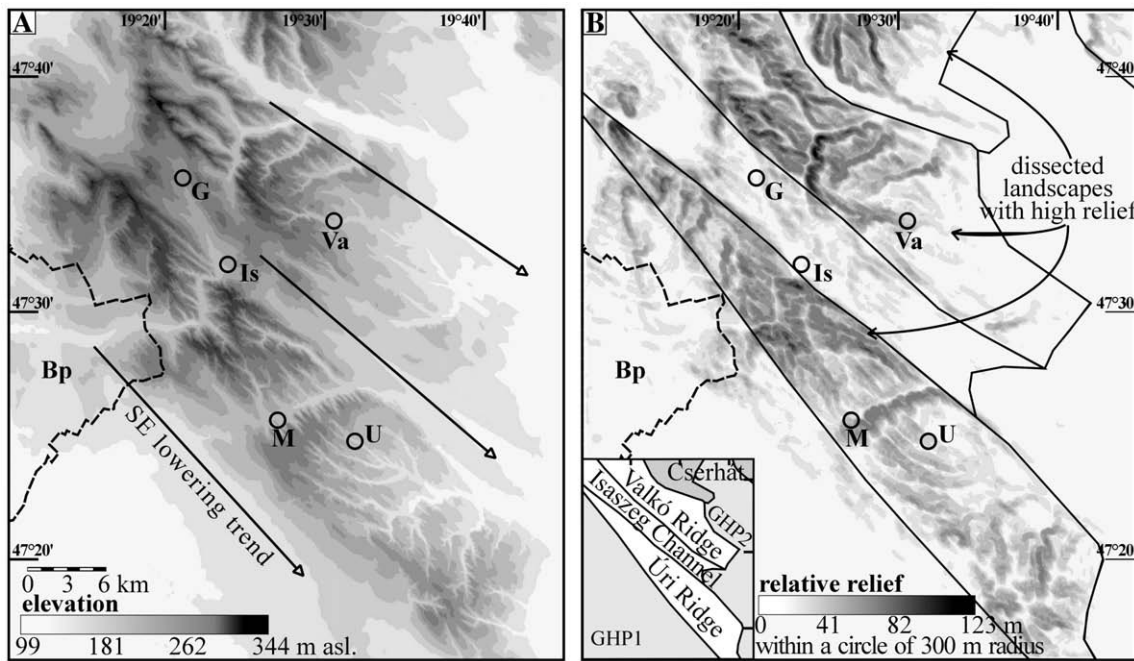


Fig. 3. Elevation characteristics of the Gödöllő Hills. A) Elevation map. Note gradual surface lowering towards the SE. B) Relative relief map. The elevation range was computed for a circular window with a radius of 300 m. Black lines delineate the topographic units. In the small inset, units of the Gödöllő Hills appear with white colour, units outside the study area have grey tone. Bp: Budapest, G: Gödöllő, Is: Isaszeg, M: Mende, U: Uri, Va: Valkó. Scale is the same for both maps.

3.1.3. Hypsometry

Hypsometry is the measurement of the elevation distribution of an area (Strahler, 1952). The topography of the catchments of the Gödöllő Hills was analysed and compared via hypsometric curves. The hypsometric curve shows the proportion of the area of a drainage basin above a certain line of elevation. It is suitable for the comparison of drainage basins of different sizes, because relative elevations (h) are plotted as proportion of the total relief (h/H) against the area above a certain line of

elevation (a) given as the proportion of the total area (a/A) of the basin (Keller and Pinter, 2002).

The hypsometric integral (I_{hyp}) is an index for characterising the shape of the hypsometric curve by calculating the area under the curve.

$$I_{hyp} = (h_{mean} - h_{min}) / (h_{max} - h_{min}) \quad (1)$$

where h_{mean} is the average height, h_{min} and h_{max} are the minimum and maximum heights of the catchment. I_{hyp} is independent of the basin size

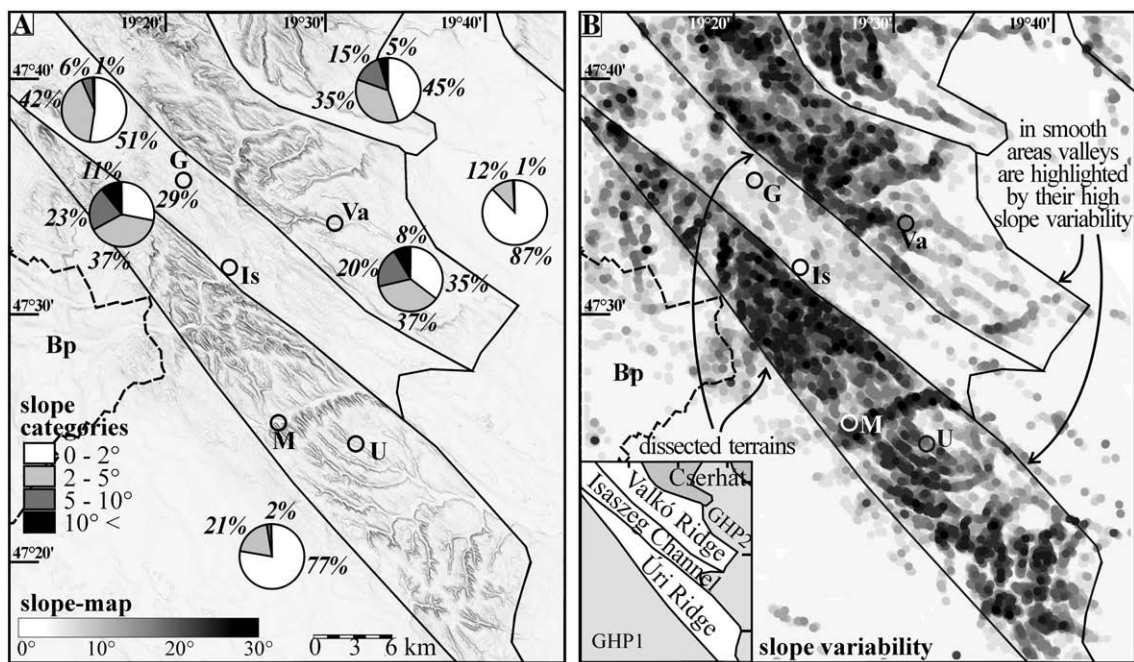


Fig. 4. Slope characteristics of the Gödöllő Hills. A) Slope map. Circle diagrams show the slope categories in the topographic units. Note that the slope conditions of the Isaszeg Channel are more similar to the lowlands than to the hills. B) Slope variability map. The slope variability was computed for a circular window with a radius of 300 m. Topographic units are outlined with black continuous lines. In the small inset units of the Gödöllő Hills appear with white colour, units outside the study area have grey tone. Bp: Budapest, G: Gödöllő, Is: Isaszeg, M: Mende, U: Uri, Va: Valkó. Scale and legend are the same for both maps.

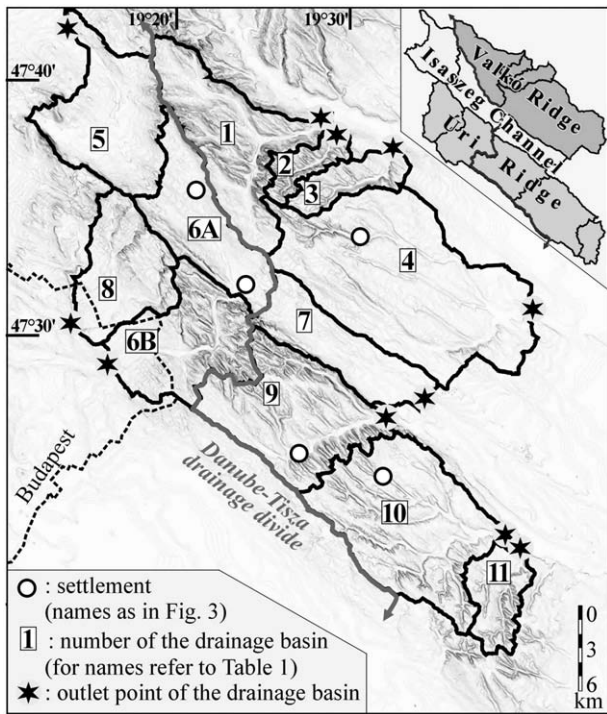


Fig. 5. Watersheds of the study area with the outlet points of the studied drainage basins and the Danube-Tisza regional drainage divide. Base map is the slope map. Inset shows the drainage basins belonging to each topographic unit.

and absolute elevation, its value varies between 0 and 1. Large values (convex upwards curve) are indicative of large areas with high elevation relative to the mean. Intermediate values (straight or S-shaped curve) suggest evenly dissected terrain and low values (concave upwards curve) usually imply large lowland areas. Extremely high or low values may indicate neotectonic deformation (Bonnet et al., 1998; Keller and Pinter, 2002), as incised valleys are typical in uplifting areas, while areas of subsidence are usually characterised by extended lowlands. On the other hand, a difference of the prevailing erosional processes may be reflected by the hypsometric curve, since fluvial incision creates dissected topography (high I_{hyp}), while deflation and fluvial aggradation have a smoothing effect (low I_{hyp}).

Table 1

Morphometric parameters of the drainage basins

nr.	main stream	topo unit	area (km ²)	perimeter (km)	min. elevation (m, asl.)	max. elevation (m, asl.)	average elevation (m, asl.)	relief (m)	std. dev. of elevation (m)	max. slope (°)	average slope (°)	std. dev. of slope (°)	I_{hyp}	L (km)	D_v (km/km ²)
1	Besnyői	VR	73.51	53.84	125	346	215.7	221	35.0	28.8	4.9	4.6	0.41	87.0	1.13
2	Nagy	VR	14.89	26.02	125	286	206.7	161	37.1	32.9	5.5	4.4	0.51	21.0	1.36
3	Sósi	VR	20.58	27.27	126	269	191.4	143	31.0	28.3	2.0	2.8	0.46	31.2	1.39
4	Kókai	VR	153.67	64.12	115	308	167.1	193	34.6	28.7	3.3	3.9	0.27	158.1	1.03
5	Szódrákosi	Ich	67.74	46.09	125	326	198.3	201	31.4	28.3	1.9	2.5	0.36	65.5	0.87
6A	Upper-Rákos	Ich	53.47	46.17	175	346	222.5	171	29.0	34.5	6.3	4.8	0.28	47.7	0.88
6B	Lower-Rákos	Ich	64.65	43.80	134	312	203.7	178	37.0	28.3	3.2	3.2	0.39	109.6	1.57
7	Felső-Tápió	Ich	45.96	38.55	136	306	179.3	170	29.1	36.0	4.0	4.1	0.25	42.2	1.12
8	Szilás	UR	50.98	34.17	144	326	221.2	182	41.4	26.6	4.1	3.6	0.42	76.4	1.45
9	Alsó-Tápió	UR	80.06	51.32	140	312	202.0	172	29.6	36.9	2.5	2.9	0.36	119.6	1.46
10	Gombai	UR	105.11	56.89	115	238	168.6	123	25.8	27.9	2.9	2.8	0.44	161.9	1.64
11	Pándi	UR	25.13	26.85	115	217	164.4	102	25.0	36.0	5.0	4.7	0.48	34.2	1.24
mean			62.9	42.9	131.2	299.3	195.1	168.1	32.2	31.1	3.8	3.7	0.39		

Catchments with smooth surface appear with dark grey background. I_{hyp} : hypsometric integral, L : total river length, D_v : valley density.

3.1.4. Derivation of the drainage network

In the Gödöllő Hills the number of the valleys with permanent waterflows is limited, therefore we use the more extended valley network to study flow directions and significance of riverine erosion (O'Callaghan and Mark, 1984; Martz and Garbrecht, 1992).

Derivation of the valley network occurred using the *StreamNetwork* tool of the *Basin* extension of the ArcView software by defining the critical source area (Mark, 1984; Jordán, 2004). Accordingly, the watercourses are defined as the cells that have an upstream drainage area larger than a user-defined threshold drainage area, which is the critical source area. The selection of an adequate threshold is crucial, because it defines the dimensions of the valleys to be analysed. When the threshold is too large, some existing valleys or upper valley reaches are neglected in the modelled drainage pattern. This problem mostly affects dissected terrains. On the other hand, where an excessively small threshold value is selected, spurious parallel channels are generated (Tribe, 1992; Jordán, 2004); a difficulty arising mostly on flat areas.

Length–azimuth rose diagrams were derived from the computed valley network to study the typical valley orientations. Directional statistics are useful in the recognition of tectonic deformation that may determine runoff directions (Centamore et al., 1996). On the other hand, directional roses are not suitable for the recognition of “irregular” – e.g. radial or centripetal – drainage patterns, river deflections, or valley-floor drainage divides, as they represent individual catchments and neglect dip directions of the valleys. Accordingly, for the recognition of irregular drainage features, indicative of neotectonic deformation (Delcaillau, 2001; Schumm et al., 2002), a qualitative analysis of the drainage pattern was also essential.

3.1.5. Topographic profiles and longitudinal valley profiles

Molin et al. (2004) used parallel topographic profiles to recognise typical valleys coincident with tectonic lines in Calabria. In our study area we study the shape of the valleys and ridges via two sets of parallel profiles running in characteristic topographic directions.

Longitudinal valley profiles (or long profiles) show the elevation of the valley floor plotted against its length. Normalized valley profiles and their concavity parameters were applied by Demoulin (1998) and by Zuchiewicz (1991, 1998) to describe geomorphic response of rivers for the differential tectonic motions of the Ardennes and of the Polish Carpathians, respectively. Normalized long profiles are dimensionless, thus allow a direct comparison of valleys with different length and absolute gradient. Distance along the valley is normalized to the total length of the valley (d/D) and elevation is normalized to the absolute

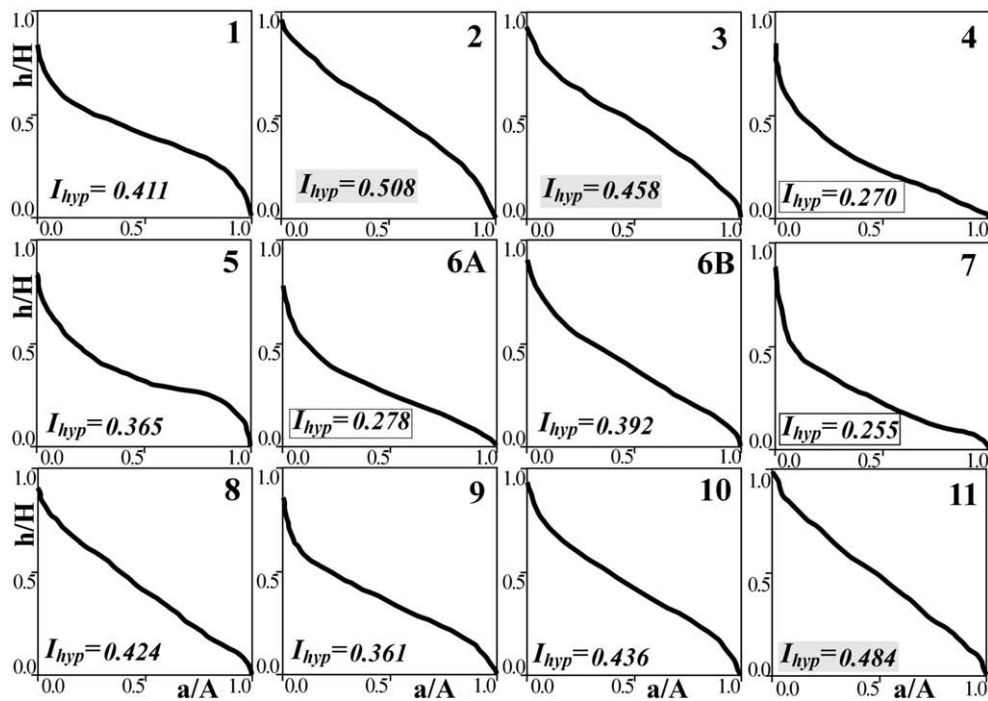


Fig. 6. Hypsometric curves of the drainage basins. Number of the basins appear in the upper right, hypsometric integral is in the bottom left corner of each plot. Smallest values (smooth landscape) are in a black frame, and highest values (dissected surface) are marked with a grey shadow. For data refer to Table 1.

gradient along the valley (e/E). Normalized profiles characterise the degree of grading of a river where z_{max} is the maximal concavity, and $\Delta d/D$ is the normalized distance of z_{max} from the source. The area on the plot between the valley profile and the straight line connecting the source and outlet of the valley is the concavity index (σ ; %). Theoretically this index is between 0.0 (0%) and 0.5 (100%). Higher values indicate a more concave profile, or a more graded river (Demoulin, 1998; Molin et al., 2004).

Graded rivers (Mackin, 1948) have a characteristic concave-upward profile, with high concavity (σ) and a maximal concavity (z_{max}) close to the source area (small $\Delta d/D$). Deviations from the graded longitudinal valley profile are indicative of external influences, such as the presence of resistant bedrock or neotectonic activity (Holbrook and Schumm, 1999; Gelabert et al., 2005).

4. Morphometric parameters of the Gödöllő Hills

4.1. Topographic units

The relief, the slope and their spatial variability proved to be suitable for the discrimination between areas of characteristically different topography in the Gödöllő Hills. Elevations (h) within the study area vary

between 99 and 344 m a.s.l., with 245 m relative relief (or relief) of the entire area. The elevation map (Fig. 3A) enhances the south-easterly regional slope of the surface with ranges smoothing into the lowland of the GHP. On the relief map (Fig. 3B) darker colours indicate high relief. The relief pattern delineates six topographic units in the studied DEM rectangle. The dissected Valkó and Úri Ridges (VR, UR) and the Cserhát

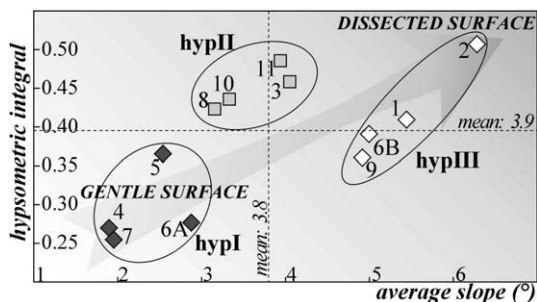


Fig. 7. Hypsometric integral of the drainage basins plotted against the average slope. Arabic numbers refer to the drainage basins. Higher average slope and hypsometric integral indicate increased surface roughness.

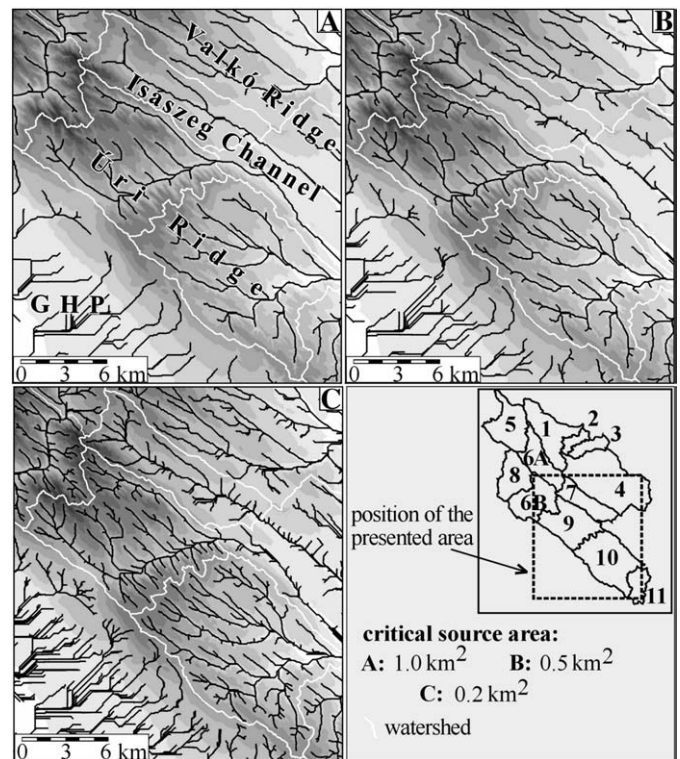


Fig. 8. Valley system with different critical source areas: A) 1.0 km², B) 0.5 km² and C) 0.2 km². Base map is the elevation map, where darker tones show higher surface. GHP: Great Hungarian Plain.

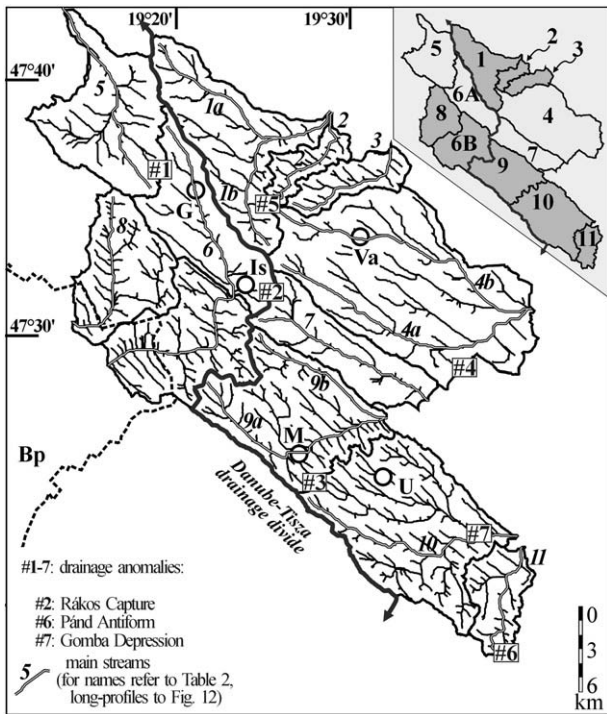


Fig. 9. Drainage network and watersheds of the study area (for names refer to Fig. 2 and Table 2). Inset shows the two groups smooth (light grey catchments) and the rugged areas (dark grey) and the numbering of the drainage basins (for names refer to Table 1). Bp: Budapest, G: Gödöllő, Is: Isaszeg, M: Mende, U: Úri, Va: Valkó.

Hills (CS) can be well distinguished from the flat areas of the Isaszeg Channel (Ich) and the GHP (GHP1 and GHP2). The area of the Gödöllő Hills is confined to three of the topographic units: the VR, UR and ICh. The other three units (CS, GHP1 and GHP2) are outside the study area, thus are beyond the scope of this analysis (Figs. 3B and 4A,B).

Slope angles vary between 0° and 30° (Fig. 4A). The slope map with darker tones of steeper slopes support the topographic division of the area: in the ICh more than 50% of the slopes are gentler than 2° and only 7% steeper than 5° , while in the VR and UR this proportion is $\sim 30\%$. Accordingly, the smooth topography of the ICh is characteristically different from that of the dissected ridges: low surface roughness of the ICh is more similar to the lowland areas (GHP1, 2). On the other hand, greater ruggedness of the VR and UR is further evidenced by the slope variability map (Fig. 4B). Towards the SE the surface roughness shows a decreasing trend, here only the valley network is highlighted by higher slope variability values. Nevertheless, in the SE part of the Úri-Ridge, an increase of surface roughness can be observed.

4.2. Drainage basins

Within the above outlined three topographic units of the Gödöllő Hills, a considerable variation of surface morphology is still observable. For the morphometric analysis, it was necessary to divide these units into smaller, more homogeneous sub-units, like drainage basins. Eleven drainage basins could be derived from the DEM of the Gödöllő Hills (Fig. 5 and Table 1). With only one exception (No. 6, Rákos Creek), the watersheds do not cross the boundaries of the topographic units, thus the catchments appeared to be suitable for a detailed study.

The drainage basin No. 6 was split into upper and lower parts. The upper reach of the stream flows southeastward within the ICh (catchment No. 6A; Fig. 5). At the village of Isaszeg the Rákos Creek abandons the ICh and cuts through the UR towards the Danube

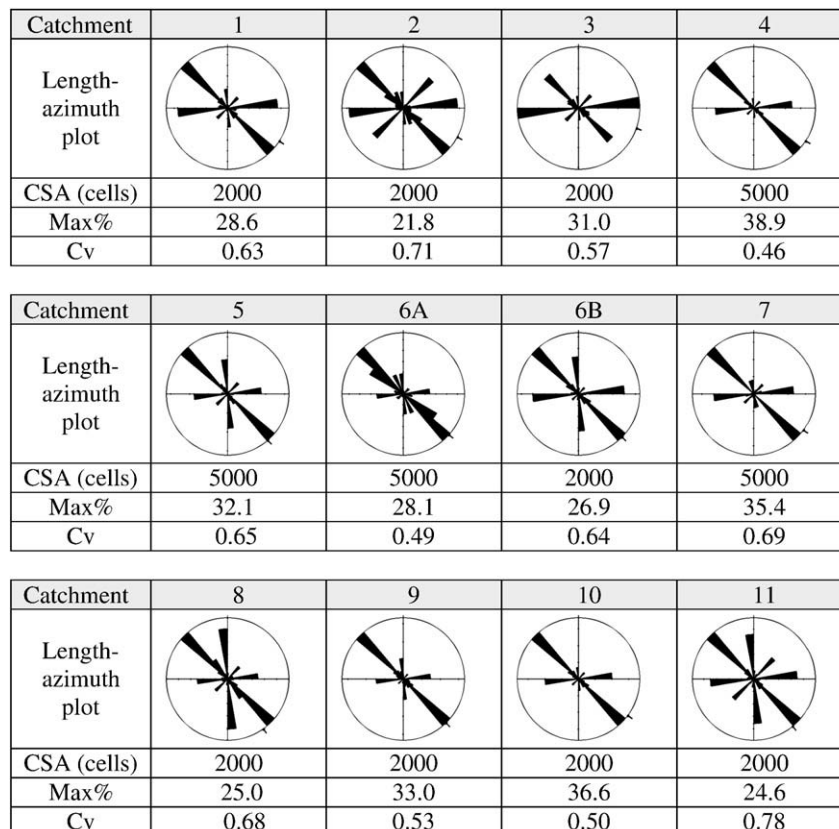


Fig. 10. Length–azimuth directional rose diagrams of the valley network for each drainage basin. CSA: critical source area in cells (1 cell = 100 m^2), Max%: The ratio of the most frequent valley direction in percentage of the total valley length, Cv: circular variance of the directional data.

(catchment No. 6B). This deflection of the Rákos Creek, the “Rákos Capture”, was first described by Leél-Össy (1953), who suggested, only on geomorphological basis, young upwarping below the drainage divide.

The hypsometric curves enabled to compare elevation conditions of the drainage basins in an objective way (Fig. 6). Drainage basins of the VR and UR (1, 2, 3, 6B, 8, 9, 10 and 11) have straight or s-shaped hypsometric curves referring to evenly dissected terrains. Concave hypsometric curves in the ICh (5, 6A and 7) and at the southeastern area of VR (4) are suggestive of large proportion of flat areas.

The hypsometric integral varies between 0.25 and 0.51, with an average of 0.39 (Fig. 6 and Table 1). Similarly to the results of Gelabert et al. (2005), we suggest that higher values of the hypsometric integral are indicative of a more dissected surface. According to this parameter, in the Gödöllő Hills the most dissected are the central part of the VR (basins 2 and 3). Interestingly, drainage basins 10 and 11, at the southeast termination of the UR and the western part of both ridges (1 and 8) also have high I_{hyp} values (>0.41). Catchments with concave hypsometric curves characterise smooth, low-relief landscapes (4, 6A and 7) having I_{hyp} values below 0.30.

Bonnet et al. (1998) used inclination of the hypsometric curves towards higher or lower elevations to assess differential uplift of the studied area. Here we use two variables, the hypsometric integral and slope values to differentiate areas of relative uplift and subsidence. In Fig. 7 three clusters could be distinguished by plotting the hypsometric integral of each drainage basin against their average slope. The “hypl” cluster (basins 4, 5, 6A and 7) has low average slope and low hypsometric integral values. These are gentle areas within the ICh and the southeastern part of the VR. The “hypll” cluster (basins 1, 2, 6B and 9) contains catchments with steep slopes and moderate to high hypsometric integral. Catchments in the “hypll” group have slightly smoother topography relative to the “hyplll” group. These clusters contain the dissected landscape of the ridges.

4.3. Direction and shape of the valleys

For an adequate derivation of the drainage network (see in 3.1 section), the study area was divided into a smooth and another, rugged part. The first group contains the catchments within the “hypl” cluster in Fig. 7; the second group consists of the “hypll” and “hyplll” clusters. In the first group the adequate critical source area of valley-definition resulted to be larger, 5000 cells (0.5 km²). In the second group a smaller value, 2000 cells (0.2 km²) proved to be the most suitable (Fig. 8A–C). Note that because of spurious channels the computed valley network could not be interpreted in the lowlands, not even using high thresholds (GHP in Fig. 8A–C). The computed valley network of the entire study area is presented in Fig. 9.

Directional roses (Fig. 10) derived from the computed valley network highlight two typical valley orientations in the study area. The primary modal orientation is NW–SE, which coincides with the overall slope of the Gödöllő Hills and also with the strike of the VR, UR and ICh. The secondary mode is oriented WSW–ENE. These two valley sets show marked differences in their shapes, as it is demonstrated by the topographic profiles of Fig. 11 in the catchment of the Alsó-Tápió Creek (No. 9). The consequent NW–SE trending valleys and ridges have symmetrical cross sections (A₁–B₃ profiles in Fig. 11; $i=1, 2$ and 3) and are frequently tributaries of the WSW–ENE trending, typically asymmetrical valleys (C₁–D₃ profiles). This latter group is characterised by long, gentle sloping northern and relatively short and steep southern valley sides.

4.4. Typical drainage patterns and river deflections

Drainage pattern analysis of Delcaillau (2001) in central Taiwan revealed the presence of a growing fault-related fold, which triggered stream captures and a gradual shift of the drainage divide. Several locations of apparent drainage pattern anomalies were also observed in the Gödöllő Hills. Because of their suspected significance as possible

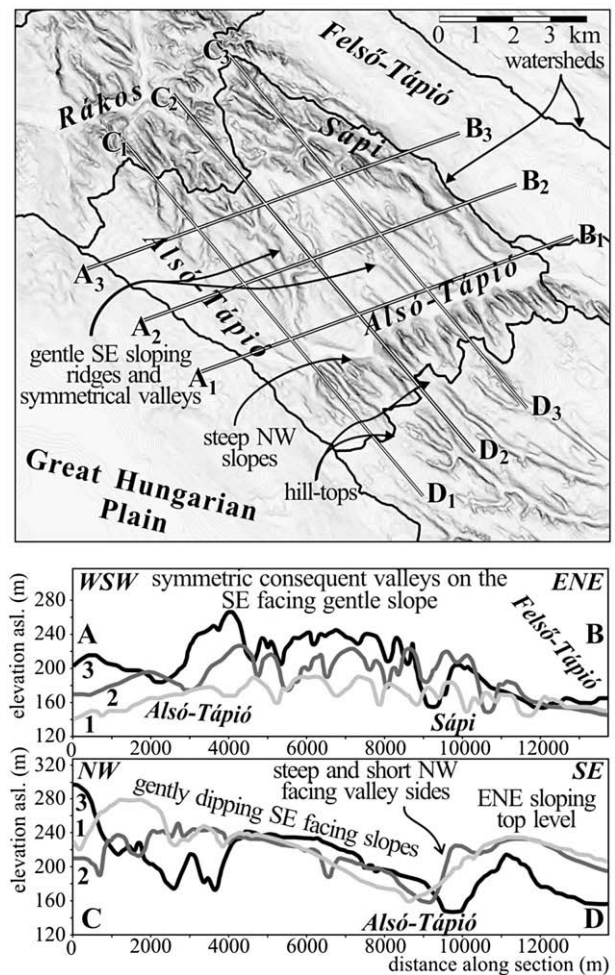


Fig. 11. Slope map and characteristic cross sections in the Alsó-Tápió drainage basin (No. 9). Offset between the parallel profiles is 2000 m. A–B profiles show the NW–SE trending symmetric valleys. C–D profiles demonstrate the asymmetry of the WSW–ENE directed Alsó-Tápió Creek.

indicators of neotectonic deformation, the drainage network was also analysed qualitatively, after the statistical evaluation of directional roses (Fig. 10).

The Isaszeg Channel is occupied by three streams with NW–SE strikes, separated by intra-valley drainage divides. The first intra-valley drainage divide is between catchments 5 and 6 (marked by “#1” in Fig. 9) and the second is the previously described Rákos Capture (“#2” in Fig. 9).

Streams drained towards the E have a typical flow direction from NW to SE. The streams No. 9a and 4a are deflected: at the southern part of their catchment they are forced to turn to the ENE and crosscut the Úri- and Valkó Ridges, respectively (drainage anomalies marked by “#3” and “#4” in Fig. 9). They collect the SE flowing consequent streams and have their outlets on the eastern side of their drainage basin. The elevation of the drainage divides at the deflections No. “#2” and “#3” is very low: their relative height does not exceed 20 m.

Radial valley networks developed in the dissected, central part of the VR among the streams No. 1b, 2, 3, 4a, and 4b (anomaly “#5” in Fig. 9). In the southeastern termination of the UR, valleys around the southeastern boundary of catchment No. 11 are also organized in a radial pattern (Pánd Antiform; “#6” in Fig. 9). The small size of the drainage areas in the southern part of this radial valley network (see the W, S, and E trending small valleys in Figs. 2 and 5) did not allow this study to include them.

Centripetal drainage pattern have developed in the UR, to the north of the Pánd Antiform (“#6”). Apparently, streams from the

surrounding areas were deviated from the consequent NW–SE trend attracted by the relative depression in the eastern part of catchment No. 10 (*Gomba Depression*; “#7” in Fig. 9).

4.5. Longitudinal valley profiles

Normalized longitudinal profiles (Fig. 12) and their concavity parameters (top left inset of Fig. 12, for a description see 3.1.5 section) were computed to recognise vertical deformations affecting the drainage network of the study area. The main stream – or in a few cases, two main

streams (1a–b, 4a–b, 9a–b) – of each drainage basin were examined (for location of the streams see Fig. 9). The concavity index (σ) varies between 19 and 56% (creeks 1a and 9b, respectively) with an average of 38% (Table 2; Fig. 12). The maximal concavity (z_{\max}) is between 0.18 (1a) and 0.49 (9b) and its position is always located in the upper half of the profiles ($\Delta d/D$ between 0.11 and 0.40; mean value of 0.27). For example, streams 4b, 7 and 9b have high z_{\max} and σ values combined with low $\Delta d/D$, suggesting that they are close to their equilibrium state.

For an objective comparison of the stream profiles and for the recognition of similarities among them, $\Delta d/D$ was plotted against z_{\max}

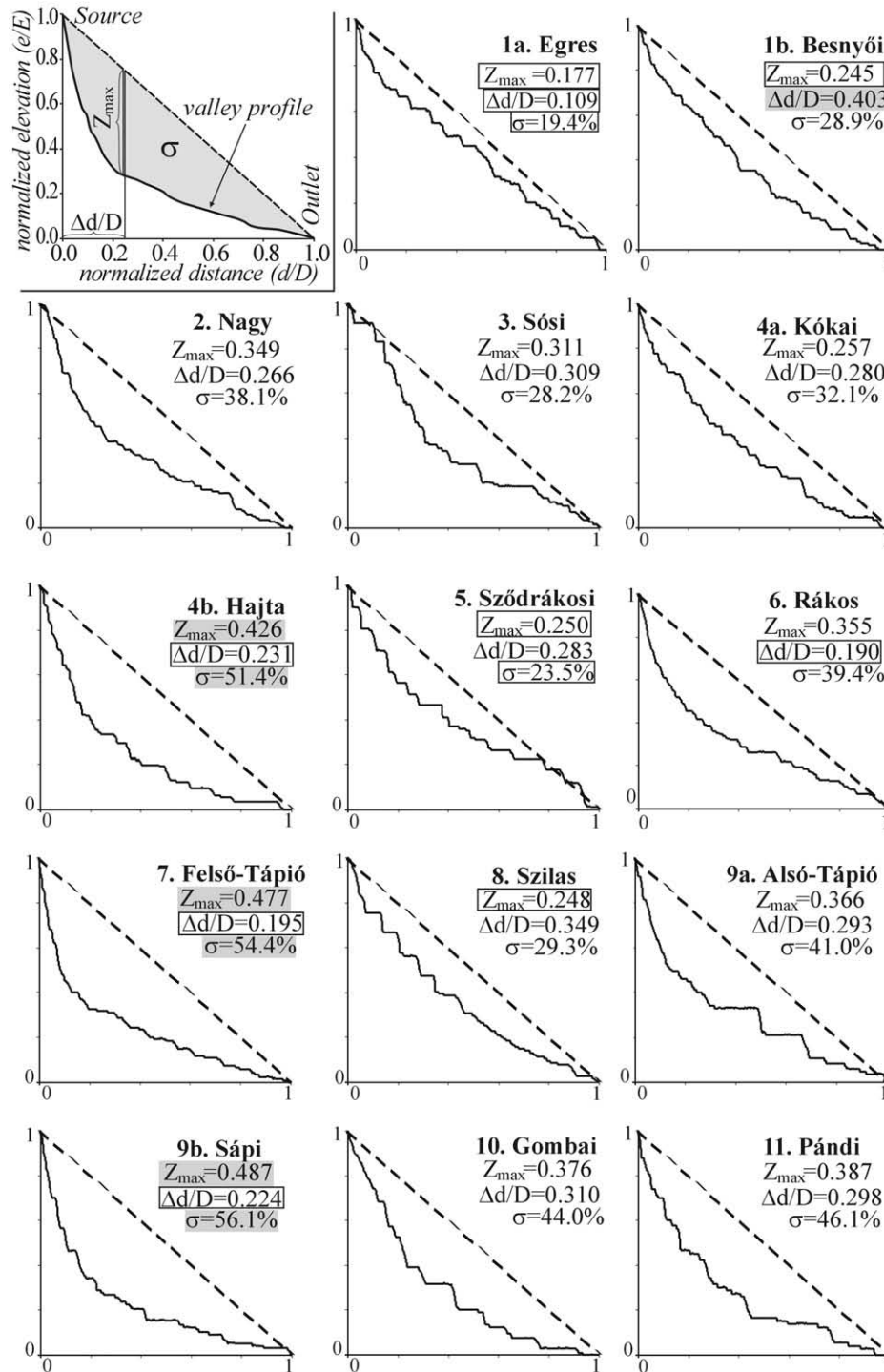


Fig. 12. Normalized longitudinal valley profiles (see map in Fig. 9). Explanation of the parameters appears in the top left corner of the figure. The concavity index (grey shadowed area, σ), the maximal concavity (z_{\max}) and its distance from the source ($\Delta d/D$) refer to the state of development of the valley. High values are highlighted with grey, low values are framed. A graded valley is characterised by small $\Delta d/D$, high σ and z_{\max} values.

Table 2
Morphometric indexes of normalized longitudinal valley profiles

nr.	name	D (km)	E (m)	G _r (m/km)	z _{max}	Δd/D	σ (%)
1a	Egres	16.71	98	5.9	0.18	0.11	19.4
1b	Besnyői	16.71	108	6.5	0.25	0.40	28.9
2	Nagy	9.62	135	14.0	0.35	0.27	38.1
3	Sósi	10.48	113	10.8	0.31	0.31	28.2
4a	Kókai	22.67	108	4.8	0.26	0.28	32.1
4b	Hajta	22.85	146	6.4	0.43	0.23	51.4
5	Sződrákosi	15.64	103	6.6	0.25	0.28	23.5
6	Rákos	28.43	156	5.5	0.36	0.19	39.4
7	Felső-Tápió	14.90	119	8.0	0.48	0.20	54.4
8	Szilas	12.09	114	9.4	0.25	0.35	29.3
9a	Alsó-Tápió	16.92	85	5.0	0.37	0.29	41.0
9b	Sápi	11.84	97	8.2	0.49	0.22	56.1
10	Gombai	17.85	105	5.9	0.38	0.31	44.0
11	Pándi	9.00	73	8.1	0.39	0.30	46.1
mean		16.12	111.5	7.5	0.34	0.27	38.0

D: valley length, E: absolute gradient, G_r: relative gradient (E/D), z_{max}: maximal concavity, Δd/D: distance of z_{max} from the source, σ: concavity index. Streams of the smooth catchments appear with dark grey background, upper reach of the Rákos creek flows through smooth area, its lower reach is crossing dissected terrain.

values. Fig. 13. allows the discrimination between three clusters of the studied valleys and one outlier (“LpI–LpIV”). The “LpI” group comprises valleys with high maximal concavity, which is situated close to the valley-head (4b, 6, 7 and 9b). These are the most graded valleys in the study area. Valleys 4b, 9b and 7 are consequent valleys not deflected from their NW–SE orientation. The upper reach of the Rákos valley (No. 6) is very similar to stream No. 7, both flowing consequently to the SE within the Isaszeg Channel. The Rákos Capture led to a rejuvenation of the long profile of the Rákos Creek but its upper reach remained almost intact. Consequently, the position of z_{max} stays close to the source (low Δd/D) and only a slight decrease of concavity of the long profile is noticeable.

“LpII” and “LpIII” clusters assemble valleys typically with one section deflected from the consequent NW–SE direction with concavity parameters around the average. The decrease of the z_{max} values of their long profiles together with an increase of the Δd/D shows a trend towards poorly graded profiles.

The “LpIV” is the isolated data point of the 1a creek, the least graded stream within the study area. Its low concavity parameters (z_{max} and σ) combined with low Δd/D are suggestive of active deformation affecting its course (Holbrook and Schumm, 1999). Our interpretation of these parameters is in accordance with other authors, who examined longitudinal profiles in different geographic settings. Rădoane et al. (2003), working in the uplifting region of the Eastern and Southern Carpathians and Gelabert et al. (2005), studying streams affected by a growing anticline developed above an inverted normal fault in Menorca, came to analogous conclusions.

5. Discussion – origin of landforms, role of fluvial erosion, deflation and structural deformation

5.1. The NW–SE trending landforms

The NW–SE-trending linear valleys, the sharp rectilinear and relatively steep slopes bounding the ICh and UR were mostly defined as tectonically controlled landforms carved by fluvial erosion (Schafarzik, 1918; Balla, 1959; Láng, 1967; Gábris, 1987; Sikhegyi, 2002). This is the primary modal orientation of the valleys demonstrated by the directional rose diagrams (Fig. 10). According to Centamore et al. (1996), who studied preferred stream orientations in central Italy, primary modal valley direction would coincide with the most typical tectonic direction in the Gödöllő Hills.

However, recent tectonic investigations of Fodor et al. (2005a,b) and Ruszkiczay-Rüdiger et al. (2007) do not support structural control on NW–SE trending landforms. Fig. 14 shows the neotectonic structures mapped on the basis of the seismic reflection data (Ruszkiczay-Rüdiger et al., 2007). The neotectonic map superposed on the digital slope map demonstrates that neotectonic structures are not reconcilable with the most frequent, NW–SE drainage orientation. Instead, the streams flowing consequently to the SE follow the dip of the Gödöllő Hills towards the subsiding GHP in the southeast.

On the other hand, there are considerable geomorphological differences between the higher, fluvially dissected ridges and the smooth ICh, which are in good agreement with the surface distribution of Quaternary sediments: the VR and UR are covered mostly by loess and fine sandy loess with several paleosol horizons, while in the ICh eolian sand is typical with some sand dunes at the drainage divide (Rákos Capture, #2; Ruszkiczay-Rüdiger, 2007). These geomorphologic and lithologic differences together with the formation of steep, linear boundaries of the topographic units cannot be interpreted as consequences of the structural tilt towards the SE.

Significant deflation in the Gödöllő Hills was first stressed by Rozlozsnik (1936) and Pávai Vajna (1941). In the western part of the Pannonian Basin, Lóczy (1913), Cholnoky (1918) and Jámboor (2002) reported significant Plio-Quaternary wind erosion. These studies, together with some recent investigations (e.g. Fodor et al., 2005a,b; Ruszkiczay-Rüdiger, 2007; Ruszkiczay-Rüdiger et al., 2007,) and the present analysis, have found evidences of deflational origin of the macro-scale landforms of the VR and UR separated by the ICh:

- (1) Westerly winds, dominant in mid-latitudes, can only enter in the Pannonian Basin where the Alpine and Carpathian mountain chains are lowered, namely in the northwest through the low topography area between the Vienna and Danube Basins (see Fig. 1). During Quaternary times, the Alps and Carpathians have already existed as elevated topographic barriers, therefore the main wind directions at that time must have been similar to today's. Besides, during glaciations the difference of temperature between the non-glaciated Pannonian Basin, and the glaciated mountains and northern Europe, must have led to a significant increase of wind power with respect to recent times. The NW–SE orientation of the sharp, rectilinear boundaries of the topographic units is in good accordance with this prevailing wind direction (Lóczy, 1913; Cholnoky, 1918; Jámboor, 2002). Additionally, eolian abrasion could be enhanced in glacial times by the coincidence of periods of reduced vegetation (Wilson et al., 2000), unable to prevent significant deflation by the increased wind power.
- (2) Spatial distribution of the most common Quaternary sediments, eolian sand and loess, suggests the presence of strong winds canalised in the ICh and a decrease of wind power on the ridges,

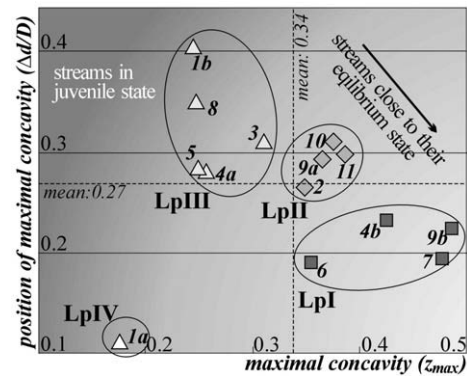


Fig. 13. Distance of maximal concavity from the source (Δd/D) plotted against maximal concavity (z_{max}) of the normalized stream profiles. Numbers refer to the valleys (see map view in Fig. 9, long profiles in Fig. 12 and data in Table 2). Grading of the valleys increases towards low Δd/D and high z_{max} values.

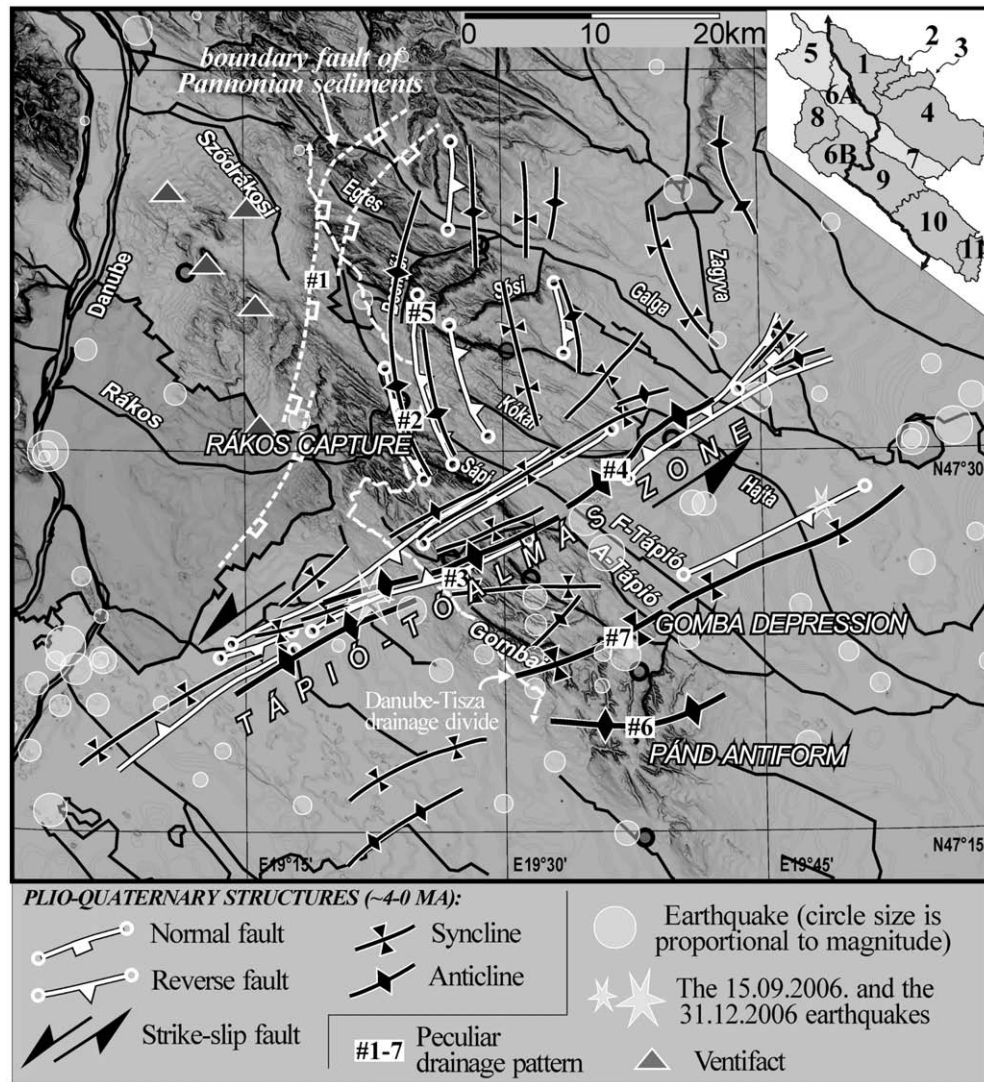


Fig. 14. Neotectonic deformation of the Gödöllő Hills (modified after Fodor et al., 2005a; Ruzsiczay-Rüdiger et al., 2007). Earthquakes are after Zsíros (2000), Tóth et al. (2007) and www.georisk.hu. Base map is the slope map, geographic names and settlements as in Fig. 2.



Fig. 15. Presence of wind-abraded rocks in the Western Pannonian Basin supporting significant Quaternary deflation in the area. Wind striation on horizontal surfaces is parallel with the prevailing NW wind direction.

typical of linear landforms shaped by uni-directional winds (Brookes, 2001).

- (3) The NW-SE-trending ICH is unusually wide with respect to modern stream flows, even if compared to the maximal modelled discharges for more humid climate periods in the area (Nováki, 1991).
- (4) Frequent occurrence of ventifacts and wind-abraded rocks in the Western Pannonian Basin (Fig. 15; Jámbor, 2002), together with pebbles with desert varnish (Schweitzer, 1997; Schweitzer and Szöör, 1997) also refer to Quaternary arid climate and strong winds (Knight, 2008). In addition, the elongated shape of the hills composed of outcropping pre-Pannonian rocks at the NW tips of the VR and UR, together with their spearhead shape typical of yardangs, support considerable deflation by uni-directional, in our case north-westerly winds (Brookes, 2001, Gutiérrez-Elroza et al., 2002).

DEM-based analysis of Bailey et al. (2007) successfully discriminated landforms of fluvial and eolian origin on large ignimbrite sheets in northern Chile. They realised that where directions of fluvial erosion and wind erosion are similar, a valley network of complex origin have developed. According to our analysis, NW-SE trending landforms of the Gödöllő Hills could

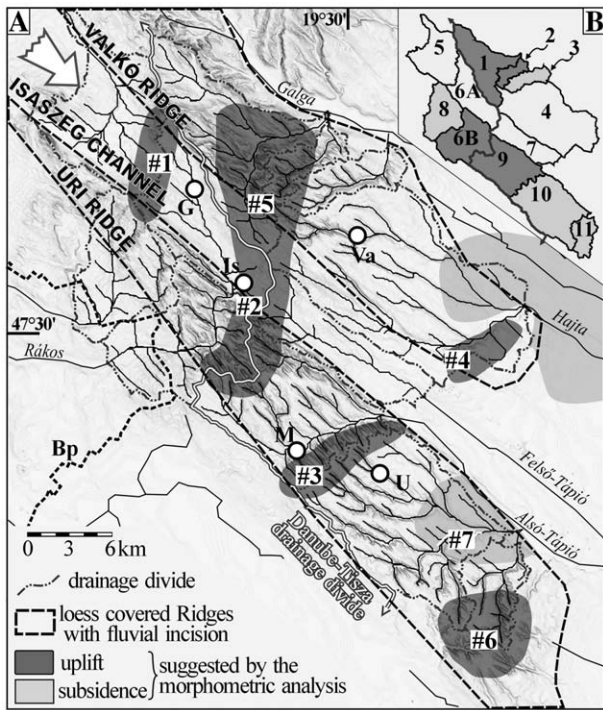


Fig. 16. Tectonic and roughness characteristics. A) Areas of relative uplift and subsidence recognised by the morphometric analysis. #1–7: locations of typical drainage patterns, Bp: Budapest, G: Gödöllő, Is: Isaszeg, M: Mende, U: Uri, Va: Valkó. B) Surface roughness of the catchments. Darker colour indicates more dissected surface.

have developed in an analogous way to the “modified” and “complex” morphology types of Bailey et al. (2007). Consequently, we suggest that the VR and UR are large-scale yardangs separated by a wind-abraded corridor, the ICh. The wind erosion had a limited effect on the surface of the yardangs, these were shaped by several phases of eolian dust accumulation, soil formation and fluvial incision.

Table 3
Neotectonic interpretation of morphometric parameters of the catchments and creeks in the Gödöllő Hills

catchment	SR	I_{hyp}	hyp I-III	D_v	creek	σ	Lp I-IV	drainage pattern type	type of deformation of the catchment
1	↑		III		1a	↓	IV	deflected (E)	uplift of S and E parts
					1b		III	radial (N)	
2	↑	↑	III		2		II	radial (NE)	uplift at the headwaters
3	↑	↑	II	↑	3		III	radial (NE)	uplift at the headwaters
4	↓	↓	I	↓	4a		III	radial (SE)/deflected (E)	uplift of the NW and SE parts
					4b	↑	I	radial/consequent (SE)	
5	↓		I	↓	5	↓	III	divergent/consequent (NW)	incision of the Danube in the W
6a	↓	↓	I	↓	6		I	consequent(SE)	uplift in the E part and incision of the Danube in the W
6b	↑		III	↑				deflected (W)	
7	↓	↓	I		7	↑	I	consequent (SE)	uplift at the headwaters
8			II	↑	8		III	deflected (W)	incision of the Danube in the W
9	↑		III	↑	9a		II	deflected (E)	uplift of the NW and SE parts
					9b	↑	I	consequent (SE)	
10			II	↑	10		II	centripetal/deflected (SE–E)	relative subsidence in the central part
11	↑	↑	II		11		II	radial (N)	uplift in the S part

Smooth areas appear with dark grey background. SR: surface roughness; I_{hyp} : hypsometric integral (high values indicate more dissected surface); hypI-III: hypsometric integral–average slope plot (Fig. 7; larger number indicates more dissected surface); σ : concavity index (Fig. 12; low values indicate streams in juvenile state); LpI-IV: position on max. concavity ($\Delta d/D$) – max. concavity (z_{max}) plot (Fig. 13; larger numbers indicate streams in juvenile state); ↑: high value; ↓: low value. Directions indicated at the “drainage pattern type” refer to the flow direction of the stream.

In the blow-out of the ICh denudation by deflation overrode fluvial erosion, thus the surface was truncated and a gentle, hummocky topography was formed (e.g. Figs. 3 and 4). At the relatively wind-shielded areas of the ridges, fluvial processes were dominant with incising streams and with minor surface denudation. Streams followed the southeast tilt of the underlying strata, towards the subsiding basin of the GHP. Accordingly, in the Gödöllő Hills fluvial erosion and deflation acted in a similar direction, which have hampered the distinction of landforms related to these processes, so far.

5.2. Formation of drainage pattern anomalies and locations of uplift and subsidence

The first intra-valley drainage divide within the ICh, between catchments No. 5 and 6, is possibly controlled by the lithologic difference along the western boundary fault of the Pannonian sediments (“#1” in Figs. 9 and 14). To the east of this fault, lithologic differences have no significant influence on drainage evolution (Ruszkiczay-Rüdiger, 2007; Ruszkiczay-Rüdiger et al., 2007). Our morphometric analysis suggests possible Quaternary deformation along this fault, as relatively high hypsometric integral values of the area (catchments No. 5 and 8) together with a divergent drainage pattern along the drainage divide are indicative of young uplift. Fig. 16 shows locations of neotectonic deformation suggested by our morphometric analysis. The most important morphometric parameters (surface roughness, hypsometry, valley patterns, and long profiles) and their neotectonic implications are summarized in Table 3.

Creeks No. 6 and 8, now tributaries of the Danube River, abandoned their original southeastward or southward strike and turned westward. We suggest that they have followed local base level drop induced by the incision of the Danube. The second valley-floor drainage divide is connected to this deviation of the Rákos Creek (No. 6, Rákos Capture; “#2” in Figs. 9, 14 and 16). In the northern segment of the drainage divide, streams No. 1b, 2, 3 4a and 4b flow radially away from an up-domed area (“#5”). The divergent drainage network, the capture of the Rákos Creek, the high relief (Fig. 3), the increased slope angles (Fig. 4) and the high surface ruggedness (Figs. 7 and 13) of the neighbouring drainage basins in the ridges (No. 1, 2, 6B and 9)

outline a N–S-trending zone of uplift (Fig. 16). Northern part of this zone is crosscut by 1a and 1b streams, characterised by longitudinal profiles of very low concavity (Figs. 9 and 12). Simoni et al. (2003) used the modification of long profiles in the Apennines to describe zones of uplift cut through by continued incision of the river. Similarly, in the northern Tien Shan, Bowman et al. (2004) described antecedent creeks keeping pace with the uplift of an anticline developed because Quaternary fault-related folding and thus impeding the anticline to become a major barrier of the drainage.

Our recent subsurface-structural studies demonstrated that in this N–S trending zone of drainage anomalies #2 and #5, deformation elements of similar strike are present (Fig. 14; Fodor et al., 2005a,b; Ruzsiczay-Rüdiger et al., 2007). On seismic reflection profiles, a number of inclined blind reverse faults were detected, whose displacement is accommodated in gentle folds near the faults or above the fault tips (Fig. 17). Although the uppermost 200 m were not properly imaged by the seismic sections, this fault-related folding could create uplift in Quaternary times, which is reflected in the observed morphotectonic indices.

This N–S trending uplifting zone in the central part of the Gödöllő Hills is also responsible for certain part of the WSW–ENE secondary modal valley direction by deflecting streams No. 1b, 2 and 6 from the NW–SE primary modal valley orientation (Figs. 9, 10 and 16). Similar response of the drainage network was described by Delcaillau (2001) in central Taiwan, who found that part of the rivers cut through the zone of uplift above growing fault-related folds and others were diverted by the emerging ridges.

Streams 4a and 9a were deflected from the consequent NW–SE strike (primary modal valley orientation), to take a WSW–ENE direction (secondary mode) to cross the VR and UR, respectively. Here they are forced to flow close to the southern rim of their catchment area (drainage anomalies “#3” and “#4” in Figs. 9, 14 and 16). The sudden change in the flow direction and asymmetric position of the trunk channel allows the diversion of these creeks in front of an emerging obstacle (e.g. an anticline) below the southeastern boundary of their catchments, as suggested by Burbank and Anderson (2001) in their theoretical model (Fig. 16).

According to our recent tectonic analysis (Fodor et al., 2005b; Ruzsiczay-Rüdiger et al., 2007; Fig. 14) the deflected sections of these creeks have developed above a WSW–ENE trending strike-slip fault zone (first recognised by Csontos and Nagymarosy, 1998; Fodor et al., 1999, 2005a,b), the Tápió-Tóalmás Zone (Ruzsiczay-Rüdiger et al., 2007). Late Pliocene–Quaternary transpression led to fault-related folding above the tip of en-echelon segments of this fault zone (Fig. 18). Holocene activity of this zone is supported by a recent (Dec.

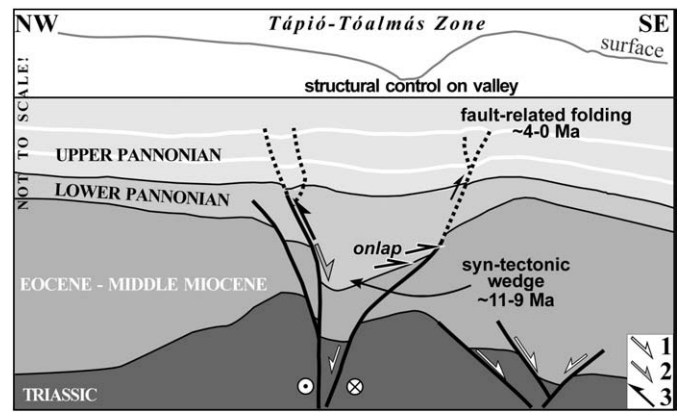


Fig. 18. Model for transpressional reactivation of the Miocene transensional Tápió-Tóalmás Zone at the drainage anomaly #3, based on seismic reflection profiles. Age of faulting is indicated: 1) early to middle Miocene, 2) late Miocene to early Pliocene, 3) late Pliocene to Quaternary.

31, 2006) earthquake (Tóth et al., 2007; Fig. 14). Surface expression of the southern branch of the Tápió-Tóalmás Zone appeared as a WSW–ENE trending zone of uplift, which caused the above described deflection of the SE flowing streams (No. 4 and 9). Accordingly, in these cases, the secondary mode of the stream directional roses (Fig. 10) is a direct consequence of the tectonic preformation of the river course. Bés de Berc et al. (2005) also described the gradual deflection of the Rio Pastaza triggered by ongoing fault growth below the Mirador anticline in the Eastern Andean Cordillera. Here, several wind gaps show the former pathways of the river. Because no wind gaps could be observed in our study area, we suggest that these creeks have passed round the emerging antiforms since the beginning of their formation.

At the southeast termination of the UR a radial stream network has developed. This feature is called Pánd Antiform (“#6” in Figs. 14 and 16). Its centre is located at the southern margin of catchment No. 11, which forms the major, northern part of this radial valley pattern. The radial valley pattern together with a relatively high surface roughness (Figs. 3, 4 and 7; Table 3), are indicative of young upwarping of the area (Keller and Pinter 2002; Fig. 16; Table 3). Our tectonic investigations (Fodor et al., 2005b; Ruzsiczay-Rüdiger et al., 2007; Fig. 16) are in accordance with the morphometric results: a roughly E–W trending anticline has been observed in the subsurface of the Pánd Antiform (Fig. 14), which could induce surface uplift and trigger the observed radial divergence and incision of the waterflows.

Between the Pánd Antiform (“#6”) and the Tápió-Tóalmás Zone (“#3” and “#4”) a centripetal drainage network, the Gomba Depression (“#7” in Figs. 14 and 16) has developed. Besides the centripetal drainage pattern open towards the E, relative subsidence of this area is suggested by its lower altitude and flat topography (i.e. decreased slope and relief; Figs. 3 and 4; Table 3). Our tectonic study revealed the presence of a syncline between the uplifting anticlines of the Tápió-Tóalmás Zone and the Pánd Antiform (Fig. 14), responsible for the relative subsidence of the Gomba Depression.

6. Conclusions

With the joint application of subsurface data on tectonic structure, morphotectonic indices and drainage pattern examination derived from digital elevation model analysis, we successfully discriminated between landforms of tectonic and non-tectonic origin. Drainage pattern anomalies showed good spatial correspondence with subsurface tectonic structures, mostly fault-related folds (Figs. 14, 17 and 18). At these locations relief and slope parameters, hypsometric integral and high surface roughness also supported neotectonic uplift. Emerging anticline crests caused river deflections (#2, #3 and #4 in Fig. 16) and divergent valley networks (#5 and #6 in Fig. 16). Strikingly low concavity of 1a

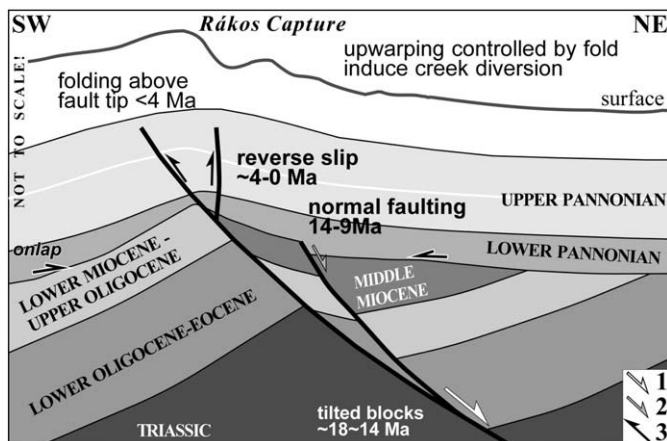


Fig. 17. Model for fault-related folding above the tip of inverted Miocene normal faults at the drainage anomaly #2, based on seismic reflection profiles. Age of faulting is indicated: 1) early to middle Miocene, 2) late Miocene to early Pliocene, 3) late Pliocene to Quaternary.

creek allowed antecedent valley evolution across the emerging fault-related fold, which provided the morphometric proof for the northern continuation of the N–S trending zone of uplift signed by the capture of the Rákos Creek and connected divergent valley patterns #2 and #5.

On the other hand, NW–SE valley orientation revealed by the directional statistics (Fig. 10), coincident with the conspicuous strike of the topographic units – the emerged and dissected Valkó and Úri Ridges and the lower and smooth Isaszeg Channel –, was proved to be of non-tectonic origin (Fig. 14). Without the joint tectonic analysis, these landforms would have easily been considered incorrectly as tectonic lineaments, and the NW–SE direction as a prevailing tectonic direction of the study area.

First conclusion of our study is that morphometric indices can predict the existence of subsurface neotectonic structures with relatively good certainty, even on a terrain of moderate deformation rate and low topography. On the other hand, at these areas exogenous forces are also capable of creating prominent, linear landforms with characteristically distinct morphometric parameters, which can easily appear as tectonic landforms. Accordingly, morphotectonic analysis is an excellent, but non-inerrable tool for the recognition of neotectonic landforms, but when completed with a subsurface tectonic study it provides reliable results on neotectonic deformation.

The second conclusion is concerning the difficulties of dating the tectonic deformation. Regarding the tectonically controlled landforms (partly) developed in Quaternary sediments, the controlling deformation should be as young as the landforms, e.g. Quaternary. Seismic profiles do not image the uppermost ~200 m of the subsurface strata; consequently the structures theoretically could die out in this thin zone, which may comprise the entire Quaternary sequence. Accordingly they do not provide information about the timing of the youngest phase of deformation. However, the combination of subsurface tectonic features and morphotectonic indices may clearly argue for tectonic structures reaching the surface, i.e. for the neotectonic activity. The “controlled test” of the composite use of morphotectonics and subsurface data presented in our study demonstrated that the morphotectonic indices allocate with a very good probability the existence of a tectonic control of a landform, despite that the tectonic feature in question may not be visible on the surface.

Finally, we provide an explanation for the origin of the macro-scale NW–SE topographic features clearly recognised by the morphometric analysis, but which proved to be of non-tectonic origin. Spatial distribution of Quaternary eolian sediments, surface dissection together with slope and relief parameters suggest eolian origin of these landforms. The fact that they cross several zones of structural deformation without any breaks in their linear edges (Fig. 16) suggests significantly increased wind power during Quaternary times. The presence of these large-scale yardangs (UR and VR) separated by a wind-blow-out channel (ICH) support that during Quaternary glaciations, cold deserts and semi-deserts could have developed in mid-latitude temperate-continental areas in Central Europe. No eolian landforms of such size – several tens of kilometres-scale – has been described from this area so far, suggesting that deflation had a significantly major role in Quaternary landscape evolution in mid-latitude temperate areas than it was assumed before.

Acknowledgements

This morphotectonic research was supported by OTKA T029798 and K062478. We are indebted to the MTA Bolyai Fellowship (L. Fodor and E. Horváth) to the ELTE PhD Fellowship and to the EUROBASIN-Marie Curie Fellowship (Zs. Ruzsiczay-R.) and to the Netherlands Research Centre for Integrated Solid Earth Sciences (ISES; L. Fodor and Zs. Ruzsiczay-R.). Síkhegyi Ferenc and Unger Zoltán (Geological Institute of Hungary) are thanked for the digital elevation data. We are also obliged to Nicholas Pinter, Piotr Migon and Takashi Oguchi for their remarks, corrections and suggestions, which helped a lot in improving the manuscript.

References

- Adediran, A.O., Parcharidis, I., Poscolieri, M., Pavlopoulos, K., 2004. Computer-assisted discrimination of morphological units on north-central Crete (Greece) by applying multivariate statistics to local relief gradients. *Geomorphology* 58, 357–370.
- Bada, G., Horváth, F., Fejes, I., 1999. Review of the present day geodynamics of the Pannonian basin: progress and problems. *Journal of Geodynamics* 27, 501–527.
- Bada, G., Horváth, F., Tóth, L., Fodor, L., Timár, G., Cloetingh, S., 2005. Societal aspects of ongoing deformation in the Pannonian region. In: Pinter, N., Greneczy, Gy., Weber, J., Medak, D., Stein, S. (Eds.), *The Adria Microplate: GPS Geodesy, Tectonics, and Hazards*. NATO ARW Series. Kluwer, Dordrecht, pp. 385–402.
- Bailey, J.E., Self, S., Wooller, L.K., Mouginis-Mark, P.J., 2007. Discrimination of fluvial and eolian features on large ignimbrite sheets around La Pacana Caldera, Chile, using Landsat and SRTM-derived DEM. *Remote Sensing of Environment* 108, 24–41.
- Balla, Gy., 1959. *Geomorphology of the loess-covered Monor-Ceglédbercel Hills*. Földrajzi Értesítő 8, 27–50 (in Hungarian).
- Bés de Berc, S., Soula, J.C., Baby, P., Souris, M., Christophoul, F., Rosero, J., 2005. Geomorphic evidence of active deformation and uplift in a modern continental wedge-top-foredeep transition: example of the eastern Ecuadorian Andes. *Tectonophysics* 399, 351–380.
- Bonnet, S., Guillocheau, F., Brun, J.-P., 1998. Relative uplift measured using river incisions: the case of the Armorican basement (France). *Comptes Rendus de l'Académie Des Sciences, Paris, Earth and Planetary Science* 327, 245–251.
- Bowman, D., Korjenkov, A., Porat, N., Czassny, B., 2004. Morphological response to Quaternary deformation at an intermontane basin piedmont, the northern Tien Shan, Kyrgyzstan. *Geomorphology* 63, 1–24.
- Brookes, I.A., 2001. Aeolian erosional lineations in the Libyan Desert, Dakhly Region, Egypt. *Geomorphology* 39, 189–209.
- Burbank, D.W., Anderson, R.S., 2001. *Tectonic Geomorphology*. Blackwell Science, Cambridge, 274 pp.
- Burrough, P.A., McDonnell, R.A., 1998. *Principles of Geographical Information Systems*. Oxford University Press, Oxford, 306 pp.
- Carter, J.R., 1988. Digital representations of topographic surfaces. *Photogrammetric Engineering and Remote Sensing* 54, 1577–1580.
- Centamore, E., Ciccacci, S., Del Monte, M., Fredi, P., Lupia Palmieri, E., 1996. Morphological and morphometric approach to the study of the structural arrangement of northeastern Abruzzo (central Italy). *Geomorphology* 16, 127–137.
- Cholnoky, J., 1918. *Hydrography of the Balaton*. A Balaton Tud. Tanulm. Eredm. I.2. Magyar Földrajzi Társ. Balaton Biz. Budapest, 319 pp. (in Hungarian).
- Csontos, L., Nagymarosy, A., 1998. The Mid-Hungarian line: a zone of repeated tectonic inversions. *Tectonophysics* 297, 51–71.
- Delcaillau, B., 2001. Geomorphic response to growing fault-related folds: example from the foothills of central Taiwan. *Geodinamica Acta* 14, 265–287.
- Demoulin, A., 1998. Testing the tectonic significance of some parameters of longitudinal river profiles: the case of the Ardenne (Belgium, NW Europe). *Geomorphology* 24, 189–208.
- Fodor, L., Csontos, L., Bada, G., Györfi, I., Benkovic, L., 1999. Tertiary tectonic evolution of the Pannonian basin system and neighbouring orogens: a new synthesis of paleostress data. In: Durand, B., Jolivet, L., Horváth, F., Séranne, M. (Eds.), *The Mediterranean Basins: Tertiary Extension within the Alpine Orogen*. Spec. Publ. Geol. Soc. London, vol. 156, pp. 295–334.
- Fodor, L., Bada, G., Csillag, G., Horváth, E., Ruzsiczay-Rüdiger, Zs., Palotás, K., Síkhegyi, F., Timár, G., Cloetingh, S., Horváth, F., 2005a. An outline of neotectonic structures and morphotectonics of the western and central Pannonian Basin. *Tectonophysics* 410, 15–41.
- Fodor, L., Bada, G., Csillag, G., Horváth, E., Ruzsiczay-Rüdiger, Zs., Síkhegyi, F., 2005b. New data on neotectonic structures and morphotectonics of the western and central Pannonian Basin. *Occasional Papers of the Geological Institute of Hungary* 204, 35–44.
- Gábris, Gy., 1987. Relationships between the orientation of drainage and geological structure in Hungary. In: Pécsi, M. (Ed.), *Pleistocene Environment in Hungary*. Akadémiai Kiadó, Budapest, pp. 183–194.
- Ganas, A., Pavlides, S., Karastathis, V., 2005. DEM-based morphometry of range-front escarpments in Attica, central Greece, and its relation to fault slip rates. *Geomorphology* 65, 301–319.
- Gelabert, B., Fornós, J.J., Pardo, J.E., Roselló, V.M., Segura, F., 2005. Structurally controlled drainage basin development in the south of Menorca (Western Mediterranean, Spain). *Geomorphology* 65, 139–155.
- Greneczy, Gy., Kenyeres, A., 2005. Crustal deformation between Adria and the European platform from space geodesy. In: Pinter, N., Greneczy, Gy., Weber, J., Medak, D., Stein, S. (Eds.), *The Adria Microplate: GPS Geodesy, Tectonics and Hazards*. Nato Science Series, vol. 61. Kluwer, Dordrecht, pp. 321–334.
- Gutiérrez-Elroza, M., Desir, G., Gutiérrez-Santolalla, F., 2002. Yardangs in the semiarid central sector of the Ebro Depression (NE Spain). *Geomorphology* 44, 155–170.
- Holbrook, J., Schumm, S.A., 1999. Geomorphic and sedimentary response of rivers to tectonic deformation: a brief review and critique of a tool for recognizing subtle epirogenic deformation in modern and ancient settings. *Tectonophysics* 305, 287–306.
- Horton, R.E., 1945. Erosional development of streams and their drainage basins: hydrophysical approach to quantitative morphology. *Bulletin of the Geological Society of America* 56, 275–370.
- Horváth, F., Cloetingh, S., 1996. Stress-induced late stage subsidence anomalies in the Pannonian Basin. *Tectonophysics* 266, 287–300.
- Jámbor, 2002. Ventifact occurrences in Hungary and their geological significance. *Földtani Közlöny* 132, 101–116 (in Hungarian with English summary).
- Jordán, Gy., 2004. *Terrain modelling with GIS for tectonic geomorphology*. Numerical methods and applications. PhD Thesis, Acta Universitatis Upsaliensis, Uppsala.

- Jordán, Gy., Meijninger, B.M.L., van Hinsbergen, D.J.J., Meulenkamp, J.E., Dijk, P.M., 2005. Extraction of morphotectonic features from DEMs: development and applications for study areas in Hungary and NW Greece. *International Journal of Applied Earth Observation and Geoinformation* 7, 163–182.
- Keller, E.A., Pinter, N., 2002. *Active Tectonics: Earthquakes, Uplift and Landscape*, 2nd ed. Prentice-Hall, Upper Saddle River. 362 pp.
- Knight, J., 2008. The environmental significance of ventifacts: a critical review. *Earth-Science Reviews* 86, 89–105.
- Láng, S., 1967. Physical geography of the Cserhát Hills. *Földr. monográfiák. Akadémiai Kiadó, Budapest.* 376 pp. (in Hungarian).
- Leél-Össy, S., 1953. Geomorphology of the surroundings of Rákóc Creek. *Földrajzi Értesítő* 2, 70–86 (in Hungarian).
- Lóczy, L., 1913. Geology and Morphology of the Surroundings of the Lake Balaton. A Balaton tud. Tanulm. Eredm. I.1. Magyar Földrajzi Társ. Balaton Biz., Budapest, 617 pp. (in Hungarian).
- Mackin, J.H., 1948. Concept of the graded river. *Geological Society of America Bulletin* 59, 463–512.
- Mark, D.M., 1984. Automatic detection of drainage networks from digital elevation models. *Cartographica* 21, 168–178.
- Martz, L.W., Garbrecht, J., 1992. Numerical definition of drainage networks and subcatchment areas from digital elevation models. *Computers and Geosciences* 18, 747–761.
- Molin, P., Pazzaglia, F.J., Dramis, F., 2004. Geomorphic expression of active tectonics in a rapidly deforming forearc, Sila Massif, Calabria, Southern Italy. *American Journal of Science* 304, 559–589.
- Nováki, B., 1991. Climatic effects on runoff conditions in Hungary. *Earth Surface Processes and Landforms* 16, 595–599.
- O'Callaghan, J.F., Mark, D.M., 1984. The extraction of drainage networks from digital elevation data. *Computer Vision, Graphics and Image Processing* 28, 323–344.
- Pávai Vajna, F., 1941. Report of my additional geologic surveys around Budapest in 1938. *Földtani Int. Évi Jel.* 1936–'38, 400–464 (in Hungarian and in German).
- Pike, R.J., 1995. Geomorphometry – progress, practice and prospect. *Zeitschrift für Geomorphologie* 36, 274–295.
- Rádoane, M., Rádoane, N., Dimitru, I., 2003. Geomorphological evolution of longitudinal river profiles in the Carpathians. *Geomorphology* 50, 293–306.
- Rónai, A., 1985. Quaternary Geology of the Great Hungarian Plain. *Geologica Hungarica, Series Geologica* 21, 446–447 (in Hungarian).
- Rozlozsnik, P., 1936. Geology of the region of Csomád, Fót and Váchartyán. *Földtani Int. Évi Jel.* 1933–'35, 851–870 (in Hungarian).
- Ruzsiczay-Rüdiger, Zs., 2007. Tectonic and climatic forcing in Quaternary landscape evolution in the Central Pannonian Basin: A quantitative, geomorphological, geochronological and structural analysis. PhD Thesis, Vrije Universiteit, Amsterdam, 149 pp.
- Ruzsiczay-Rüdiger, Zs., Fodor, L., Horváth, E., 2007. Neotectonic and landscape evolution of the Gödöllő Hills, Central Pannonian Basin. *Global and Planetary Change* 58, 181–196.
- Schafarzik, F., 1918. Paleohydrography of the Danube at Budapest. *Földtani Közlöny*, 48, 184–200 and 207–225. (in Hungarian and German).
- Schumm, S.A., Dumont, J.F., Holbrook, J.M., 2002. *Active Tectonics and Alluvial Rivers*. Cambridge Univ. Press, Cambridge, p. 276.
- Schweitzer, F., 1997. On late Miocene–early Pliocene desert climate in the Carpathian Basin. *Zeitschrift für Geomorphologie Neue Folge Supplementband* 110, 37–43.
- Schweitzer, F., Szöör, Gy., 1997. Geomorphological and stratigraphical significance of Pliocene red clay in Hungary. *Zeitschrift für Geomorphologie Neue Folge Supplementband* 110, 95–105.
- Scott, A.T., Pinter, N., 2003. Extraction of coastal terraces and shoreline-angle elevations from digital terrain models, Santa Cruz and Anacapa Islands, California. *Physical Geography* 24, 271–294.
- Síkhegyi, F., 2002. Active structural evolution of the western and central parts of the Pannonian basin: a geomorphological approach. *EGU Stephan Müller Special Publication Series* 3, 203–216.
- Simoni, A., Elmi, C., Picotti, V., 2003. Late Quaternary uplift and valley evolution in the Northern Apennines: Lamone catchment. *Quaternary International* 101–102, 253–267.
- Strahler, A.N., 1952. Hypsometric (area–altitude) analysis of erosional topography. *Bulletin of the Geological Society of America* 63, 1117–1142.
- Strahler, A.N., 1957. Quantitative analysis of watershed geomorphology. *Eos Transactions of the American Geophysical Union* 38, 913–920.
- Székely, B., 2001. On the surface of the Eastern Alps – a DEM study. *Tübinger Geowissenschaftliche Arbeiten, Reihe A* 60, 1–124.
- Szentes, F., 1943. *Geology of the Surroundings of Aszód*. Magyar tájak földtani leírása, Budapest. 70 pp. (in Hungarian and in German).
- Tóth, L., Mónus, P., Zsíros, T., Bus, Z., Kiszely, M., Czifra, T., 2007. *Yearbook of Hungarian Earthquakes 2006*. Georisk, Hungarian Academy of Sciences, Geodesy and Geophysics Research Institute, Budapest. 80 pp.
- Tribe, A., 1992. Automated recognition of valley lines and drainage networks from grid digital elevation models: a review and a new method. *Journal of Hydrology* 139, 263–293.
- Uhrin, A., Sztanó, O., 2007. Reconstruction of Pliocene fluvial channels feeding Lake Pannon (Gödöllő Hills, Hungary). *Geologica Carpathica* 58, 291–300.
- Wilson, J.P., Gallant, J.C., 2000. *Terrain Analysis, Principles and Applications*. Wiley, New York. 480 pp.
- Wilson, R.C.L., Drury, S.A., Chapman, J.L., 2000. *The Great Ice Age. Climate Change and Life*. The Open University, London. 267 pp.
- Zsíros, T., 2000. Seismicity and Earthquake-hazard in the Carpathian Basin. *Hungarian Earthquake Catalogue 456-1995*. HAS, Geological Research Group, Seismological Observatory, Budapest (in Hungarian).
- Zuchiewicz, W., 1991. On different approaches to neotectonics: a polish Carpathians example. *Episodes* 14, 116–124.
- Zuchiewicz, W., 1998. Quaternary tectonics of the Outer West Carpathians, Poland. *Tectonophysics* 297, 121–132.